2011 American Control Conference
on O'Farrell Street, San Francisco, CA, USA
June 29 - July 01, 2011

Correlation of Multiple Singular Observations and Initial State Estimation by Means of Probability Distributions of High Codimension

Kohei Fujimoto and Daniel J. Scheeres

Abstract— **Optical observations of Earth-orbiting particles are singular in that multiple observations are required to determine the state of the object. It is generally uncertain, however, whether two arbitrary singular observations are of the same object, and solving this problem can be computationally intensive. In this paper, we propose a technique of correlating multiple singular observations and providing an initial estimate of the observed object's state by means of probability distributions in state space, provided the distributions have high-codimension.**

I. Introduction

Situational awareness of Earth-orbiting particles such as active satellites and space debris is highly important for future human activities in space. Presently, over 300,000 particles have been estimated to exist, and over 80,000 observations are made per day [11]. Observations are made either by radar or optical sensors. For optical observations, which are usually made for objects in medium Earth orbit (MEO) and geostationary orbit (GEO), only the angles and angular rates of the track can be determined. That is, the range and range-rate remain largely unknown. Therefore, optical observations are *singular* in that in order to determine the orbit of the observed object, multiple observations must be combined. In other words, a singular observation is consistent with an infinite number of states. It is generally uncertain, however, whether two arbitrary tracks are of the same object. This is the crux of the *too short arc* (TSA) correlation problem, and the solution can be computationally intensive. Milani et al. have proposed a solution for heliocentric orbits where each track is expressed in a 4-dimensional quantity called the *attributable vector*, and by placing a few physical constraints, they restrict the range and range-rate to a region called the *admissible region* [7]. Discretized points on the admissible region are referred to as *Virtual Debris* (VD) *particles*. Tommei et al. expanded this method to Earth orbiting objects [12]. Maruskin et al. introduced another method that uses maps of the admissible region in Delaunay orbit element space [6]. Outside of the realm of astrodynamics, this problem has been considered in multiple target tracking using bearing only sensors, such as multiple hypothesis tracking [5], [10]. However, these techniques require *a priori* information or a reference state, a Gaussian assumption on the error distribution, or great computational power.

In this paper, we propose a technique of correlating multiple singular observations and simultaneously providing an initial estimate of the observed object's state by means of probability distribution functions (pdf's) in state space. We first generalize the concept of admissible regions to an n-dimensional state space with only $m < n$ independent observable variables. Each observation is expressed as a pdf in state space, which is physically an $n - m$ dimensional manifold embedded in n-space. Note that this pdf is generated from physical constraints on the system and does not require us to assume any particular distribution (Section II). The region of intersection between multiple pdf's gives a state estimate that is consistent with all observations. When we expect that the uncertainty is dominant only in a few coordinate directions, as is true for optical observation data, we find that the pdf's can be well approximated as having a high codimension with respect to the state space. Then, the likelihood that two pdf's of unrelated observations intersect is very low (Section III). An example of our method is discussed in the end, where we correlate simulated optical observations of objects in MEO and GEO. It demonstrates the ability of our method to correlate observations and provide an initial state estimate without any *a priori* information. (Section IV).

II. The Generalized Admissible Region

We generalize the idea of the admissible region for a system with n state variables $\mathbf{X}$ but where only $m < n$ independent observable variables and c parameters are available [3], [6], [7], [12]. Per observation, the system is underdetermined.

Definition 2.1: A *singular* observation is one that is consistent with an infinite number of states.

Definition 2.2: An *attributable vector* $\mathfrak{X}$ is an $m + c$ dimensional vector that contains all observable variables and parameters for a given singular observation.

Suppose there exists a one-to-one transformation $T(\tau, t_0)$ that maps the observable variable space at time t_0 to the state space at time τ:

$$T(\tau, t_0) : \langle \mathbf{x}(t_0), \mathfrak{X}(t_0) \rangle \rightarrow \langle \mathbf{X}(\tau) \rangle, \tag{1}$$

where $\mathbf{x} = (x_1, x_2, \ldots, x_{n-m})^{\mathrm{T}}$ is an $n - m$ dimensional vector of undetermined observation variables. To linearize

This research is supported by AFOSR grant number FA9550-08-1-0460

K. Fujimoto is a graduate student of the Department of Aerospace Engineering Sciences at The University of Colorado at Boulder, 166 ECEE, 431 UCB, Boulder, CO, 80309-0431 USA

D. J. Scheeres is the A. Richard Seebass Chair Professor of the Department of Aerospace Engineering Sciences at The University of Colorado at Boulder, 611 ECOT, 429 UCB, Boulder, CO, 80309-0429 USA

this transformation, we find matrix $\Phi(\tau, t_0)$ such that:

$$\Phi(\tau, t_0) = \frac{\partial \mathbf{X}(\tau)}{\partial \mathbf{x}(t_0)}. \quad (2)$$

Then, to first order we have

$$\delta\mathbf{X}(\tau) = \Phi(\tau, t_0)\delta\mathbf{x}(t_0), \quad (3)$$

where δ denotes a small deviation from some reference point.

For some attributable vector $\mathfrak{X}$, we can assume different particular values of $\mathbf{x}$ to complete the state description. However, it is often the case that not all of these states are relevant for any given application.

Definition 2.3: Given some set of criteria C, the *admissible region* A is a closed compact set in the $n - m$ dimensional undetermined observation variable space such that all of the physically relevant states are contained within the interior of this region.

Definition 2.4: A probability distribution function (pdf) $F_{\mathfrak{X}}(\mathbf{x})$ may be assigned to an attributable vector $\mathfrak{X}$ such that the probability p that the observed object exists in region $B \subset A$ is

$$p = \int_B F_{\mathfrak{X}}(\mathbf{x})\mathrm{d}x_1\mathrm{d}x_2 \ldots \mathrm{d}x_{n-m}. \quad (4)$$

Note that $\int_A F_{\mathfrak{X}}(\mathbf{x})\mathrm{d}x_1\mathrm{d}x_2 \ldots \mathrm{d}x_{n-m} = 1$.

Corollary 2.1: The map of the admissible region to the full state space can be regarded as an $n - m$ dimensional manifold embedded in an n dimensional space, assuming the errors in the observable variables and parameters are much smaller than the uncertainty in the undetermined observation variable. One example is an optical observation where the angle and angle-rates of the observed object are more well-observed than range and range-rate [6]. Consequently, the map of $F_{\mathfrak{X}}(\mathbf{x})$ to the state space $T(\tau, t_0) \circ F_{\mathfrak{X}}(\mathbf{x})$ is also an $n - m$ dimensional distribution.

III. Combining Probability Distributions

We now consider how to relate pdfs from multiple singular observations, and in the event that they do, compute a state estimate via Bayes' theorem. For this, we first discuss the spatial relationship between multiple pdf's in state space.

Definition 3.1: A singular observation is *consistent* with some region V in state space if:

$$\int_V \{\mathcal{T}(\tau, t_0) \circ F_{\mathfrak{X}}(\mathbf{x})\}\, \mathrm{d}X_1\mathrm{d}X_2 \ldots \mathrm{d}X_n > 0, \quad (5)$$

where $\mathcal{T}(\tau, t_0)$ maps the pdf from time t_0 to τ.

Note that, in general, to map a pdf, one must solve the Fokker-Planck differential equations. For deterministic Hamiltonian systems, however, the total time derivative of a pdf is constant, independent of whether the potential field is time invariant. As a consequence, $\mathcal{T}(\tau, t_0) = T(\tau, t_0)$ [8].

Definition 3.2: An observation and an object are *related* over V if the observation is consistent with the same region V in state space as the object resides in. Similarly, two observations are related over V if they are consistent with the same region V in state space.

Definition 3.3: Let P be a probability measure, and event $E_O(V, \tau)$ be one where some object O of interest exists in region V in state space at time τ. Then, we define some pdf $g_O(\mathbf{X}, \tau)$ such that:

$$P[E_O(V, \tau)] = \int_V g_O(\mathbf{X}, \tau)\mathrm{d}X_1\mathrm{d}X_2 \ldots \mathrm{d}X_n. \quad (6)$$

Similarly, let event $E_{\{r\}}(V, \tau)$ be one where some observation information series $\{r\}$ is consistent with region V assuming all information has been dynamically evolved to a common epoch τ. Then, we define some pdf $f_{\{r\}}(\mathbf{X}, \tau)$ such that:

$$P[E_{\{r\}}(V, \tau)] = \int_V f_{\{r\}}(\mathbf{X}, \tau)\mathrm{d}X_1\mathrm{d}X_2 \ldots \mathrm{d}X_n. \quad (7)$$

Both f and g can originate from admissible region maps $\mathcal{T}(\tau, t_0) \circ F_{\mathfrak{X}}(\mathbf{x})$ or be generated *a priori*. We will drop the τ notation unless we want to emphasize the epoch time.

Lemma 3.1: Suppose f and g are manifolds embedded in an n-dimensional state space such that

$$\dim(f) + \dim(g) < n. \quad (8)$$

Then the probability that f and g will intersect randomly is 0.

Proof: This is a direct result of the theory of general position [2]. ■

Corollary 3.1: For an object O and information series $\{r\}$ that satisfies (8), if event x_r^O is one where $\{r\}$ is related to O, the conditional probability

$$P[x_r^O | E_O(V)] = \int_V f_{\{r\}}(\mathbf{X})\mathrm{d}X_1\mathrm{d}X_2 \ldots \mathrm{d}X_n \quad (9)$$

for any choice of V.

Proof: From Lemma 3.1 and given O exists in region V, if both $\{r\}$ and O lie in any V they are most likely related. That is, whether $\{r\}$ and O are related depends only on whether $\{r\}$ is consistent with V. Thus, $P[x_r^O|E_O(V)] = P[E_{\{r\}}(V)] = \int_V f_{\{r\}}(V)\mathrm{d}X_1\mathrm{d}X_2 \ldots \mathrm{d}X_n$. ■

Corollary 3.2: For an object O and information series $\{r\}$ that satisfies (8), if the two are related then

$$\int f_{\{r\}}(\mathbf{X})g_O(\mathbf{X})\mathrm{d}X_1\mathrm{d}X_2 \ldots \mathrm{d}X_n > 0, \quad (10)$$

where the integral is taken over the entire state space. The converse is almost always true.

Proof: If the pdf's intersect at $\mathbf{X}$=$\mathbf{q}$, then the integral of $f \cdot g$ over any ϵ-ball centered at $\mathbf{q}$ must be non-zero. The converse is a consequence of Lemma 3.1.

Now, from Corollary 2.1, the pdf's are locally homeomorphic to $\mathbb{R}^{n-m}$, where n is the dimension of the state space and m is the dimension of the observable variable space. Then, we can describe points near some $\mathbf{X}^*$ on f as follows:

$$\mathbf{X} = \mathbf{X}^* + s_1\mathbf{v}_1 + s_2\mathbf{v}_2 + \cdots + s_{n-m}\mathbf{v}_{n-m}, \tag{11}$$

where $\{\mathbf{v}\}$ are some independent bases of $\mathbb{R}^{n-m}$, and $s_j \in \mathbb{R}$ for $j = 1, 2, \ldots, n-m$. Similarly on g,

$$\mathbf{Y} = \mathbf{Y}^* + t_1\mathbf{u}_1 + t_2\mathbf{u}_2 + \cdots + t_{n-m}\mathbf{u}_{n-m}. \tag{12}$$

Then, locally, the intersection of the manifolds is described as:

$$\mathbf{X} = \mathbf{Y} \tag{13}$$

$$\Leftrightarrow \mathbf{z} = \mathrm{M}\,\mathbf{s}, \tag{14}$$

where

$$\mathrm{M} = \begin{bmatrix} \mathbf{v}_1 & \mathbf{v}_2 & \cdots & \mathbf{v}_{n-m} & -\mathbf{u}_1 & \cdots & -\mathbf{u}_{n-m} \end{bmatrix} \tag{15}$$

$$\mathbf{s} = \begin{bmatrix} s_1 & s_2 & \cdots & s_{n-m} & t_1 & \cdots & t_{n-m} \end{bmatrix}^T \tag{16}$$

$$\mathbf{z} = \mathbf{X}^* - \mathbf{Y}^*. \tag{17}$$

For f and g that satisfy (8), M cannot be inverted since M is not full rank. By taking the pseudoinverse we find:

$$\tilde{\mathbf{s}} = (\mathrm{M}^T\mathrm{M})^{-1}\mathrm{M}^T\mathbf{z} \tag{18}$$

$$= \tilde{\mathrm{M}}\,\mathbf{z}. \tag{19}$$

For the two pdf's to intersect at $\mathbf{s} = \tilde{\mathbf{s}}$, it is necessary that $\mathbf{z}$ have components of 0 in the direction of the null-space bases of $\tilde{\mathrm{M}}$. This condition acts as constraints on the local orientation of the manifolds that must be met for them to intentionally intersect. For instance, if $\tilde{\mathrm{M}}$ is rank $2(n-m)$, then $\ker(\tilde{\mathrm{M}}) = n - \{2(n-m)\} = 2m - n$, so there are $2m-n$ constraints on $\mathbf{z}$. If $\tilde{\mathrm{M}}$ is rank $2(n-m)-1$, then one pair of bases $(\mathbf{u}_j, \mathbf{v}_k)$ is linearly dependent. This dependency creates 1 constraint for $\tilde{\mathrm{M}}$ in addition to the $2m-n+1$ constraints for $\mathbf{z}$ for a total of $2m-n+2$ constraints on (18). In conclusion, at a local level, more and more constraints must be met for f and g to intersect.

Proposition 3.1: For two pdf's that satisfy (8) and intersect, the local dimension $d_\times$ of the intersection is:

$$d_\times = 2(n-m) - \mathrm{rank}(\tilde{\mathrm{M}}). \tag{20}$$

Proof: At the intersection of the local Euclidian space equivalents of pdf's f and g, the two spaces must share bases. Therefore, $d_\times$ is the number of dependent column pairs in M. Note that $\min(\mathrm{rank}(\tilde{\mathrm{M}})) = n-m \Rightarrow \max(d_\times) = n-m$, since we assumed $\{\mathbf{v}\}$ and $\{\mathbf{u}\}$ both spanned $\mathbb{R}^{n-m}$. ■

Theorem 3.1: Given object O and observation $\{r\}$ are related, we can define some pdf:

$$h_O(\mathbf{X}, \tau) = \frac{f_{\{r\}}(\mathbf{X}, \tau) g_O(\mathbf{X}, \tau)}{\int f_{\{r\}}(\mathbf{X}, \tau) g_O(\mathbf{X}, \tau) \mathrm{d}X_1 \mathrm{d}X_2 \ldots \mathrm{d}X_n} \tag{21}$$

such that

$$P[E_O(V, \tau) | x_r^O] = \int_V h_O(\mathbf{X}, \tau) \mathrm{d}X_1 \mathrm{d}X_2 \ldots \mathrm{d}X_n, \tag{22}$$

where the integral in (21) is taken over the entire state space.

Proof: Apply Bayes' theorem with (9) [9]. Note that from (10), (21) is well defined. ■

If (8) is true, then by solving for h we correlate prior information regarding O with the new information $\{r\}$ and find where in the state space O is likely to exist. $P[E_O(V) \cap E_{\{r\}}(V)]$ includes cases when x_r^O does not hold in its universal set, which we know are trivial from Lemma 3.1. Therefore, we'd like to add x_r^O as a condition to filter out such trivial cases. Now, as long as h is well defined, then from Corollary 3.2 the condition x_r^O is almost always valid. On the contrary, if h is not defined, then we conclude O and $\{r\}$ were most likely unrelated. Finally, if more observations become available, we let h from the previous step be the new g. The process can be repeated as necessary.

For ease of computation, we discretize the state space into uniform subspaces.

Definition 3.4: A *bin* is a unit of discretization. Each bin is assigned an index vector $\mathbf{i} = (i_1, i_2, \ldots, i_n)^{\mathrm{T}} \in \mathbb{N}^n$ such that $i_j = 1, 2, \ldots, M_j$ for some $j = 1, 2, \ldots, n$, where $\mathbf{M} = (M_1, M_2 \ldots, M_n) \in \mathbb{N}^n$ prescribes the maximum index in each coordinate direction. Then,

$$i_j = \begin{cases} \mathrm{floor}\left[M_j(X_j - X_{j,min})/(X_{j,max} - X_{j,min}) + 1\right] & \text{(23a)} \\ M_j & \text{(23b)} \end{cases}$$

where (23a) is when $X_j \neq X_{j,max}$, (23b) is when $X_j = X_{j,max}$. $X_{j,max}$ and $X_{j,min}$ are the maximum and minimum possible values of $\mathbf{X}$ in the j-direction as determined by the discretization, respectively. Furthermore, the *index scaled state space* $\bar{\mathbf{X}}$ is defined such that:

$$\bar{\mathbf{X}} = K\mathbf{X} + \mathbf{k}, \tag{24}$$

where K is some diagonal matrix and $\mathbf{k} \in \mathbb{R}^n$ such that

$$\mathbf{i} = \mathrm{floor}(\bar{\mathbf{X}}). \tag{25}$$

Corollary 3.3: A singular observation is *consistent* with some bin $\mathbf{i}$ if (5) is true for when $V = \mathbf{i}$; i.e. when V occupies the same region as $\mathbf{i}$. An observation and an object O are *related* if the observation is consistent with the same bin as the object resides in. Two observations are related if they are consistent with the same bin.

Corollary 3.4: Let event $E_O(\mathbf{i}, \tau)$ be one where object O resides in bin $\mathbf{i}$ at time τ. Then, we define some pdf $g'_O(\mathbf{i}, \tau)$ such that:

$$P[E_O(\mathbf{i}, \tau)] = g'_O(\mathbf{i}, \tau) = \int_{V=\mathbf{i}} g_O(\mathbf{X}, \tau) \mathrm{d}X_1 \mathrm{d}X_2 \ldots \mathrm{d}X_n. \tag{26}$$

Similarly, let event $E_{\{r\}}(\mathbf{i}, \tau)$ be one where information series $\{r\}$ is consistent with bin $\mathbf{i}$. Then, we define some pdf $f'_{\{r\}}(\mathbf{i}, \tau)$ such that:

$$P[E_{\{r\}}(\mathbf{i}, \tau)] = f'_{\{r\}}(\mathbf{i}, \tau) = \int_{V=\mathbf{i}} f_{\{r\}}(\mathbf{X}, \tau) \mathrm{d}X_1 \mathrm{d}X_2 \ldots \mathrm{d}X_n. \tag{27}$$

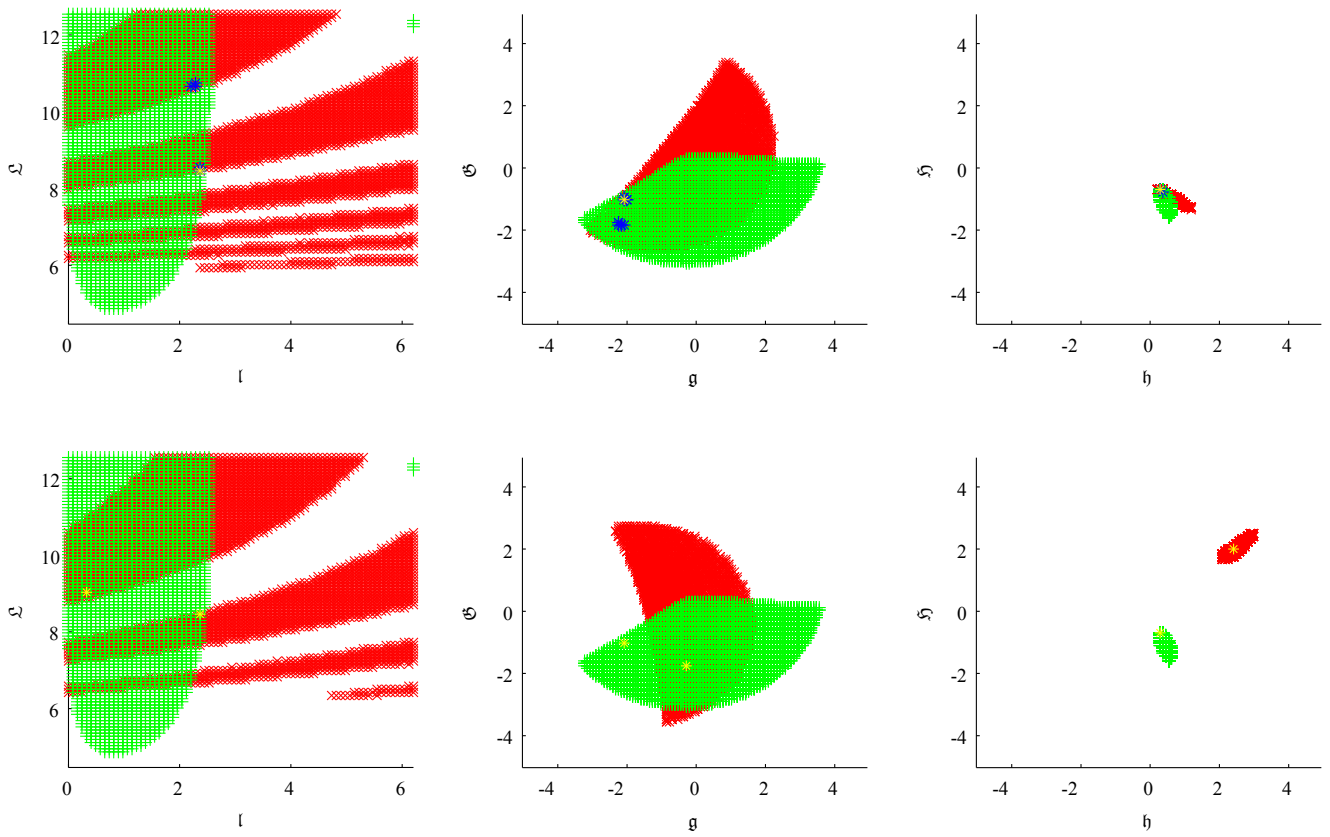

Fig. 1. Projections of probability distributions when correlating observations of the same object (top) and a different object (bottom). Length units in Earth radii, time units in hours, mass units in kilograms.

Finally, we define some pdf $h'_O(\mathbf{i},\tau)$ such that:

$$P[E_O(\mathbf{i},\tau)|x_r^O] = h'_O(\mathbf{i},\tau) = \frac{f'_{\{r\}}(\mathbf{i},\tau)g'_O(\mathbf{i},\tau)}{\Sigma_{\mathbf{j}} f'_{\{r\}}(\mathbf{j},\tau)g'_O(\mathbf{j},\tau)}. \quad (28)$$

Proof: These are the discretized equivalents of Definition 3.3 and Theorem 3.1. ■

IV. Examples

In this section, we discuss correlation and initial orbit determination results for optical observation simulations of mainly MEO and GEO objects [13]. The purpose of this example is to show that our method is capable of correlating observations of multiple objects and obtaining an initial state estimates of these objects without *a priori* information or assumption of a particular statistical distribution, and that the computational load is moderate.

We extracted 8 objects from the two-line element (TLE) catalog, which contains orbital information for all known and tracked Earth-orbiting objects, to obtain a sample set [1]:

- 3 objects in GEO,
- 1 object in a Molniya orbit,
- 2 object in an eccentric MEO orbit,
- 1 object in a circular MEO orbit, and
- 1 GPS satellite.

We further generated one random object in the MEO region that is not included in the TLE catalog for a total of 9 objects. The orbital parameters of each object is given in Appendix I.

We simulated 3 batches of zero-error observations of right ascension (α), declination (δ), and their time derivatives for all 9 objects. Thus $\mathfrak{X} = (\alpha, \delta, \dot{\alpha}, \dot{\delta}, \mathrm{h}, \Theta, \phi)$, where (Θ, ϕ) is the angular position and h is the altitude of the observation point. We then generated admissible regions for each observations based on criterion set C in Fujimoto, et al. [3]. The undetermined observation variables are $\mathbf{x} = (\rho, \dot{\rho})$, or topocentric range and range-rate. Again, the error-free approximation is good since the state uncertainty due to observation error is much less than that due to the uncertainty in range and range-rate [6]. Each batch was separated temporally by approximately 10 hours. We assumed no *a priori* information regarding the observed objects, and thus used a uniform initial pdf. We chose the Poincaré orbital element space $\mathbf{X} = (\mathfrak{L}, \mathfrak{l}, \mathfrak{G}, \mathfrak{g}, \mathfrak{H}, \mathfrak{h})$ as our state space variables since they are the non-singular canonical counterpart to the equinoctial orbit elements. They can be naturally grouped into two by their coordinate-momenta symplectic pairs [6], [13]. The non-singular property assures that the mapping function $T(\tau, t_0)$ is well defined everywhere. The symplectic paring is useful when projecting 6-dimensional distributions onto 2-

TABLE I

LIST OF ALL 3-OBSERVATION SERIES THAT RESULTED IN $h > 0$ USING A UNIFORM INITIAL PDF (LEFT) AND THE TLE AS THE INITIAL PDF (RIGHT).

	Uniform			**Preconditioned**	
$\{r\}$	Overlap bins	Contains true state	$\{r\}$	Overlap bins	Contains true state
GEO1-GEO1-GEO1	4	YES	GEO1-GEO1-GEO1	2	YES
GEO2-GEO2-GEO2	3	YES	GEO2-GEO2-GEO2	2	YES
GEO3-GEO3-GEO3	6	YES	GEO3-GEO3-GEO3	2	YES
MOL1-MOL1-MOL1	1	YES	MOL1-MOL1-MOL1	1	YES
EM1-EM1-EM1	2	YES	EM1-EM1-EM1	1	YES
EM2-EM2-EM2	9	YES	EM2-EM2-EM2	1	YES
CM1-CM1-CM1	5	YES	CM1-CM1-CM1	1	YES
GPS1-GPS1-GPS1	7	YES	GPS1-GPS1-GPS1	1	YES
RAN1-RAN1-RAN1	8	YES			

dimensional subspaces for visualization. Refer to Appendix II for the definition of Poincaré variables. We implemented two-body dynamics for this example:

$$\mathbf{X}(t) = (\mathfrak{L}_0, \mathfrak{l}_0 + \mu^2/\mathfrak{L}_0^2, \mathfrak{G}_0, \mathfrak{g}_0, \mathfrak{H}_0, \mathfrak{h}_0), \tag{29}$$

where subscript 0 denotes the state at time t_0. Since two-body dynamics is non-dissipative, from Definition 3.1, propagating the admissible region is equivalent to propagating the state space. As a consequence, admissible regions can be propagated linearly via matrix $\Phi(\tau, t_0)$ in order to reduce computational burden [4].

Per observation, an admissible region was computed and mapped linearly to the discretized Poincaré space. The discretization was such that:

$$\mathbf{X}_{min} = (4.4621, 0, -5.0241, \ldots \\ -5.0241, -5.0241, -5.0241)^{\mathrm{T}} \tag{30}$$

$$\mathbf{X}_{max} = (12.6206, 6.2832, 5.0241, \ldots \\ 5.0241, 5.0241, 5.0241)^{\mathrm{T}}, \tag{31}$$

and $\mathbf{M} = (100, 77, 123, 123, 123, 123)^{\mathrm{T}}$ for a total of 1.7624×10^{12} bins. These values were chosen so that the algorithm detects all objects in the TLE catalog with reasonable memory burden; future work is to choose the discretization resolution more optimally in order to improve correlation and state estimation accuracy.

Fig. 1 is a graphical representation of the process explained in Section III for two observations. The red and green regions each represent a pdf based on an admissible region that has been dynamically evolved to a common epoch (i.e. pdf's f and g). The propagation has "shredded" the red pdf in the $\mathfrak{L}$-$\mathfrak{l}$ plane [6]. The blue region is the combined distribution (i.e. pdf h). The yellow asterisk is the true state of the observed object. Note that although these distributions are plotted on 2-dimensional subspaces, the correlation was conducted in the full 6-dimensional Poicaré space. When correlating two observations of the same object, we see that $h > 0$ for a very small region of the state space; for this particular example, $h > 0$ for 11 bins. Furthermore, the true state is included in the region in state space where $h > 0$. Therefore, the state estimate is good. On the other hand, when two observations are of different objects, $h = 0$ for the entire state space. This result allows us to conclude that the two observations are unrelated.

Our correlation process performed well for all $9^3 = 729$ combinations of 3-observation series: all related observations resulted in $h > 0$ for a region of no more than 9 bins that contained the true state, and all unrelated observations produced $h = 0$ for the entire state space. On a dual-core Intel Xeon workstation running MATLAB, each linear admissible region map $\Phi(\tau, t_0)$ took 20 to 40 minutes. This time is orders of magnitude less than the direct non-linear map $T(\tau, t_0)$, which took several days. In addition, since each subspace map is independent of each other, the process can be parallelized easily. With the same setup, each correlation run took approximately 10 minutes.

If we wish to further reduce the region over $h > 0$ as well as reduce computation time, we can assume *a priori* that all observed objects were included in either the TLE catalog or some debris distribution model instead of the uniform distribution assumption we made for this example. Then, the admissible region maps are "pre-conditioned" to exclude unrealistic objects. We ran a test case where we pre-conditioned the admissible regions using the TLE catalog object distribution. The orbit of all objects extracted from the TLE catalog were determined to within 2 bins. The randomly generated object, however, did not correlate with the TLE data. Although its orbit could not be estimated, the algorithm succeeds in suggesting that this object has yet to be catalogued. Correlation times were reduced to 1 to 2 minutes. All correlation results are summarized in TABLE I.

V. CONCLUSIONS

In this paper, we discussed methods of correlating multiple singular observations as well as providing initial state estimates using pdf's in state space with high codimension. We outlined the algorithm that incorporates Bayes' rule in both continuous and discretized space. An application to optical observations of MEO and GEO objects demonstrated how our method accurately solves for an initial state estimate in a reasonable time frame.

Future work will incorporate real-world observation data with noise and error. This task will entail optimizing the discretization resolution that better matches the distribution of debris objects in Earth-orbit. We also plan on investigating

analytical arguments regarding the relative angular position of two observations and the number of intersections the 2 associated pdf's could have.

Appendix I
Orbital Parameters for Objects in the Example

The classical and Poincaré orbital elements of all 9 objects in our simulation sample set are listed below. Earth radius is denoted as $\mathrm{r_E}$.

- GEO
  1) (a [$\mathrm{r_E}$], e, i [rad], Ω [rad], ω [rad], M [rad])
     = (6.6102, 0.0003, 0.0002, 3.1274, 2.3294, 5.7226),
     ($\mathfrak{L}$ [$\mathrm{r_E}^2$/hour], $\mathfrak{l}$ [rad], $\mathfrak{G}$ [$\mathrm{r_E}$/hour$^{1/2}$], $\mathfrak{g}$ [$\mathrm{r_E}$/hour$^{1/2}$],
     $\mathfrak{H}$ [$\mathrm{r_E}$/hour$^{1/2}$], $\mathfrak{h}$ [$\mathrm{r_E}$/hour$^{1/2}$])
     = (11.4721, 4.8962, 0.0006, 0.0006, −0.0000, −0.0006)
  2) (6.6109, 0.0003, 0.0009, 5.9501, 2.9681, 5.8729),
     (11.4727, 2.2247, −0.0005, −0.0009, 0.0010, 0.0029)
  3) (6.6109, 0.0001, 0.0001, 3.0902, 4.2464, 6.1176),
     (11.4727, 0.8879, −0.0003, 0.0001, −0.0000, −0.0002)
- Molniya
  1) (4.1971, 0.7154, 1.1204, 0.8126, 5.1137, 0.1671),
     (9.1414, 6.0934, 0.8200, 2.1991, −1.9501, 1.8469)
- Eccentric MEO
  1) (3.6573, 0.7123, 0.3106, 1.0976, 1.6080, 5.9942),
     (8.5333, 2.4166, −0.9526, −2.0447, −0.6739, 0.3451)
  2) (4.1472, 0.5529, 1.2347, 5.5811, 2.4137, 4.8996),
     (9.0868, 0.3281, −1.7237, −0.2444, 2.0573, 2.4323)
- Circular MEO
  1) (3.9994, 0.0006, 1.1284, 4.9148, 4.2128, 2.9461),
     (8.9234, 5.7905, −0.0005, −0.0017, 3.1297, 0.6421)
- GPS satellite
  1) (4.1645, 0.0048, 0.9599, 2.7242, 3.6934, 2.5851),
     (9.1057, 2.7195, −0.0019, 0.0143, −1.1296, −2.5474)
- Random Uncatalogued MEO object
  1) (4.5000, 0.3000, 0.7854, 1.5708, 1.5708, 1.5708),
     (9.4655, 4.7124, −0.0000, −0.9338, −2.2999, 0.0000)

Appendix II
Definition of Poincaré Orbital Elements

The Poincaré orbital elements are defined here in terms of a transformation from the topocentric spherical coordinates. The transformation is performed in several steps. First, from topocentric spherical coordinates to geocentric Cartesian coordinates:

$$T_1 : \langle \rho, \dot{\rho}, \mathfrak{X} \rangle \rightarrow \langle x, y, z, \dot{x}, \dot{y}, \dot{z} \rangle,$$

then to orbital elements [13]:

$$T_2 : \langle x, y, z, \dot{x}, \dot{y}, \dot{z} \rangle \rightarrow \langle a, e, i, \Omega, \omega, M \rangle,$$

where a is the semi-major axis, e is the eccentricity, $i \in [0, \pi]$ is the inclination, $\Omega \in [-\pi, \pi]$ is the longitude of the ascending node, $\omega \in [-\pi, \pi]$ is the argument of periapsis, and $M \in [-\pi, \pi]$ is the mean anomaly. Finally, we transform the orbital elements to Poincaré variables:

$$T_3 : \langle a, e, i, \Omega, \omega, M \rangle \rightarrow \langle \mathfrak{L}, \mathfrak{l}, \mathfrak{G}, \mathfrak{g}, \mathfrak{H}, \mathfrak{h} \rangle,$$

which are defined as:

$$\begin{aligned}
\mathfrak{l} &= \Omega + \omega + M & \mathfrak{L} &= \sqrt{\mu a} \\
\mathfrak{g} &= \sqrt{2\mathfrak{L}\left(1 - \sqrt{1 - e^2}\right)} \cos(\omega + \Omega) & \mathfrak{G} &= -\mathfrak{g} \tan(\omega + \Omega) \\
\mathfrak{h} &= \sqrt{2\mathfrak{L}\sqrt{1 - e^2}\,(1 - \cos i)} \cos\Omega & \mathfrak{H} &= -\mathfrak{h} \tan\Omega,
\end{aligned}$$

where μ is the standard gravitational parameter.

References

[1] Satellite situation report. Report, HQ AFSPC/XOCS. Retrieved from `http://www.space-track.org/` on August 10, 2009.

[2] J. S. Carter. *How Surfaces Intersect in Space: An introduction to topology*. World Scientific, Singapore, second edition, 1995. pp. 277.

[3] K. Fujimoto, J. M. Maruskin, and D. J. Scheeres. Circular and zero-inclination solutions for optical observations of earth-orbiting objects. *Celestial Mechanics and Dynamical Astronomy*, 106(2):157–182, 2010.

[4] K. Fujimoto and D. J. Scheeres. Correlation of optical observations of earth-orbiting objects by means of probability distributions. 2010. Presented at the *2010 AIAA/AAS Astrodynamics Specialist Conference*.

[5] F. Gustafsson, F. Gunnarsson, N. Bergman, U. Forssell, J. Jansson, R. Karlsson, and P. Nordlund. Particle filters for positioning, navigation, and tracking. *IEEE Transactions on Signal Processing*, 50(2):425437, 2002.

[6] J. M. Maruskin, D. J. Scheeres, and K. T. Alfriend. Correlation of optical observations of objects in earth orbit. *Journal of Guidance, Control and Dynamics*, 32(1):194–209, 2009.

[7] A. Milani, G. Gronchi, M. Vitturi, and Z. Knežević. Orbit determination with very short arcs. i admissible regions. *Celestial Mechanics and Dynamical Astronomy*, 90:57–85, 2004.

[8] R. S. Park and D. J. Scheeres. Nonlinear mapping of gaussian statistics: Theory and applications to spacecraft trajectory design. *Journal of Guidance, Control and Dynamics*, 29(6):1367–1375, 2006.

[9] S. J. Press. *Subjective and Objective Bayesian Statistics: Principles, Models, and Applications*. John Wiley & Sons, Inc., Hoboken, NJ, second edition, 2003.

[10] D. R. Reid. An algorithm for tracking multiple targets. *IEEE Transactions on Automatic Control*, AC-24(6):843–854, 1979.

[11] A. Rossi. The earth orbiting space debris. *Serb. Astron. J.*, (170):1–12, 2005.

[12] G. Tommei, A. Milani, and A. Rossi. Orbit determination of space debris: admissible regions. *Celestial Mechanics and Dynamical Astronomy*, 97:289–304, 2007.

[13] D. Vallado. *Fundamentals of Astrodyamics and Applications*. Microcosm Press, Hawthorne, CA, third edition, 2007. pp. 119.